The EMBO Journal Vol.17 No.13 pp.3651–3659, 1998

A glutamic finger in the guanine nucleotide exchange factor ARNO displaces Mg^{2+} and the β-phosphate to destabilize GDP on ARF1

Sophie Béraud-Dufour, Sylviane Robineau, Pierre Chardin, Sonia Paris, Marc Chabre, Jacqueline Cherfils[1] and Bruno Antonny[2]

CNRS, Institut de Pharmacologie Moléculaire et Cellulaire, 660 route des lucioles, 06560 Valbonne and [1]CNRS, Laboratoire d'Enzymologie et Biochimie Structurales, 91198 Gif-sur-Yvette, France

[2]Corresponding author
e-mail: antonny@ipmc.cnrs.fr

S.Béraud-Dufour and S.Robineau contributed equally to this work

The Sec7 domain of the guanine nucleotide exchange factor ARNO (ARNO-Sec7) is responsible for the exchange activity on the small GTP-binding protein ARF1. ARNO-Sec7 forms a stable complex with the nucleotide-free form of [Δ17]ARF1, a soluble truncated form of ARF1. The crystal structure of ARNO-Sec7 has been solved recently, and a site-directed mutagenesis approach identified a hydrophobic groove and an adjacent hydrophilic loop as the ARF1-binding site. We show that Glu156 in the hydrophilic loop of ARNO-Sec7 is involved in the destabilization of Mg^{2+} and GDP from ARF1. The conservative mutation E156D and the charge reversal mutation E156K reduce the exchange activity of ARNO-Sec7 by several orders of magnitude. Moreover, [E156K]ARNO-Sec7 forms a complex with the Mg^{2+}-free form of [Δ17]ARF1-GDP without inducing the release of GDP. Other mutations in ARNO-Sec7 and in [Δ17]ARF1 suggest that prominent hydrophobic residues of the switch I region of ARF1 insert into the groove of the Sec7 domain, and that Lys73 of the switch II region of ARF1 forms an ion pair with Asp183 of ARNO-Sec7.

Keywords: ARF/ARNO/G protein/guanine nucleotide exchange factor/Sec7 domain

Introduction

ARF1 is a small GTP-binding protein involved in vesicular trafficking (Moss and Vaughan, 1995). ARF1 is distantly related to Ras and to other small GTP-binding proteins but adopts a similar fold. However, ARF1 shows two structural elements that have no counterpart in Ras: an extra β strand (β2E) and an N-terminal helix (Amor *et al*., 1994; Greasley *et al*., 1995) (Figure 1). The N-terminal helix is amphipathic and myristoylated, and is involved in the GTP-dependent interaction of ARF1 with membrane lipids (Franco *et al*., 1993; Antonny *et al*., 1997). The function of strand β2E is unknown. In Ras, the cognate region is the effector loop or switch I region (Milburn *et al*., 1990; Pai *et al*., 1990). Whether strand β2E is also a switch must await further description of the ARF1-GTP structure, but the fact that it displays several exposed hydrophobic residues and is responsible for the dimerization of ARF1-GDP in some crystal forms (Amor *et al*., 1994; Greasley *et al*., 1995) suggests a role in protein–protein interactions.

Like all G proteins, ARF1 switches from an inactive GDP-bound state to an active GTP-bound state upon the catalytic action of a guanine nucleotide exchange factor (GEF). The yeast protein Gea1 and the human protein ARNO were the first GEFs described for ARF1 (Peyroche *et al*., 1996; Chardin *et al*., 1996). These two proteins are different in size and share no amino acid homology except for a central domain of ~200 amino acids, termed the Sec7 domain. This domain was first identified in Sec7, the product of one of the genes involved in secretion in yeast, and is found in all recently discovered GEFs for ARF such as cytohesin, Grp1 and p200 (Meacci *et al*., 1997; Morinaga *et al*., 1997; Klarlund *et al*., 1998). As expected, the Sec7 domain is responsible for the exchange activity on ARF1. All constructs of ARNO that encompass this domain are active on ARF1 (Chardin *et al*., 1996). These constructs are also active on a truncated form of ARF1 that lacks the first 17 residues ([Δ17]ARF1), suggesting that the Sec7 domain of ARNO (ARNO-Sec7) interacts with the core domain of ARF1 and not with the myristate or the N-terminal amphipathic helix (Paris *et al*., 1997). A soluble 1:1 complex between ARNO-Sec7 and [Δ17]ARF1, in which [Δ17]ARF1 has lost its GDP, can be isolated by gel filtration (Paris *et al*., 1997). This 'empty' complex is a stable intermediate state which is observed or suspected for all mechanisms of GEF-catalyzed nucleotide exchange (Jacquet *et al*., 1995; Klebe *et al*., 1995a). In addition, two protein–lipid interactions act coordinately to facilitate the interaction of ARNO with ARF1 at the membrane surface: the binding of the pleckstrin homology (PH) domain of ARNO to phosphatidylinositol bisphosphate (PIP_2) and the weak interaction of full-length myristoylated ARF1-GDP with the bilayer (Chardin *et al*., 1996; Paris *et al*., 1997).

The crystal structure of the Sec7 domain of ARNO has been solved recently (Cherfils *et al*., 1998; Mossessova *et al*., 1998). It consists of 10 helices (numbered A–J) and shows a striking hydrophobic groove (Figure 1). Hydrophobic residues from helices F and G form the bottom of the groove while hydrophobic residues from helix H and hydrophilic residues of loop F–G form the two facing sides of the groove. Loop F–G and helix H correspond to two highly conserved motifs that are found in the sequence of all members of the Sec7 family (Chardin *et al*., 1996). As shown by site-directed mutagenesis, the groove and its adjacent edges form the active site of the Sec7 domain. Several mutations in the hydrophilic F–G loop (R152E, E156K) and in helix αH (M194A, N201A) impair the exchange activity of ARNO-Sec7 on full-length myristoylated ARF1 (Cherfils *et al*., 1998).

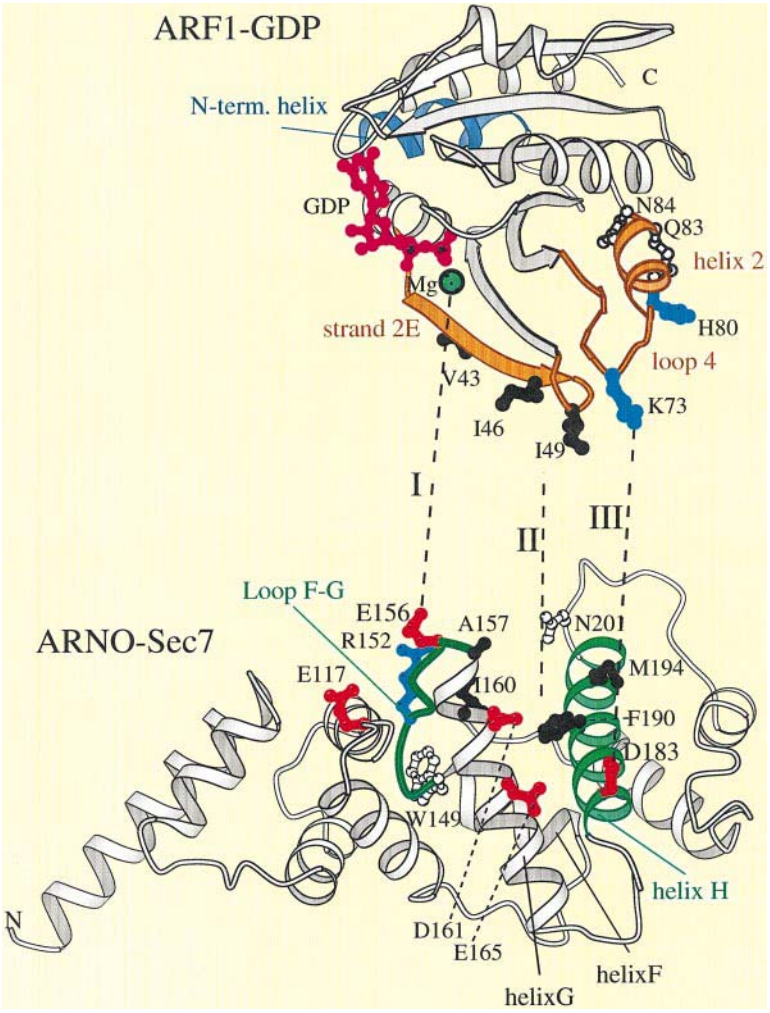

Fig. 1. Ribbon drawings of ARF1-GDP and the Sec7 domain of ARNO. All residues that have been mutated and some residues discussed in the text are shown. For all residues, the following color code was used: white (polar), black (hydrophobic), red (acidic) and blue (basic). The switch regions of $ARF1_{GDP}$ are shown in orange and the N-terminal helix is shown in light blue. Helix H and the hydrophilic F–G loop of ARNO-Sec7 which define the two facing edges of the groove of this domain are shown in green. The three vertical dashed lines indicate the three contacts between ARNO-Sec7 and ARF1-GDP that were studied: (I) the catalytic attack of the Mg^{2+} and the β-phosphate of ARF1-bound GDP by the carboxylate group of Glu156 of ARNO-Sec7; (II) a hydrophobic contact between residues Ile46 and Ile49 of strand β2E (ARF1) and the groove of the Sec7 domain; and (III) an ion pair interaction between Lys73 (ARF1) and Asp183 (ARNO-Sec7). This figure was generated with MOLSCRIPT (Kraulis, 1991) using the coordinates of ARF1-GDP (Amor *et al*., 1994) and ARNO-Sec7 (Cherfils *et al*., 1998).

In this study, the interface between ARF1 and the Sec7 domain of ARNO was explored further by site-directed mutagenesis. Several mutations on [Δ17]ARF1 and ARNO-Sec7, including conservative and charge reversal mutations, reveal some key structural or functional interactions between ARNO-Sec7 and ARF1. This leads to a model for the ARF1–ARNO-Sec7 interface and for the mechanism of ARNO-Sec7-catalyzed nucleotide exchange on ARF1.

Results

The conservative E156D mutation reduces the exchange activity of the Sec7 domain of ARNO by a factor of 400

We have previously identified several residues of ARNO-Sec7 that are important for its guanine nucleotide exchange activity on full-length myristoylated ARF1 by site-directed mutagenesis (Cherfils *et al*., 1998). All critical residues belong to the edges of the characteristic groove of ARNO-Sec7 (Figure 1). The most severe defect in the exchange activity of ARNO-Sec7 was observed when Glu156 was mutated to lysine (Cherfils *et al*., 1998). This prompted us to examine the effect of the conservative E156D mutation, which shortens the side chain, but leaves the carboxylate group intact. The E156D mutation reduced the exchange activity of ARNO-Sec7 on [Δ17]ARF1 by a factor of 400 compared with a factor of 1200 for the charge reversal E156K mutation (Figure 2). Strikingly, the E156D and E156K mutations have a much more dramatic effect than mutations at other positions (Figure 2B). This suggests a key role for the long, negatively charged side chain of Glu156 in the mechanism of Sec7-catalyzed nucleotide exchange on ARF1.

The E156K mutant of ARNO-Sec7 binds to the Mg^{2+}-free form of [Δ17]ARF1-GDP but does not induce the release of the bound GDP

We examined the ability of [E156K]ARNO-Sec7 to interact with [Δ17]ARF1 by gel filtration. [E156K]ARNO-

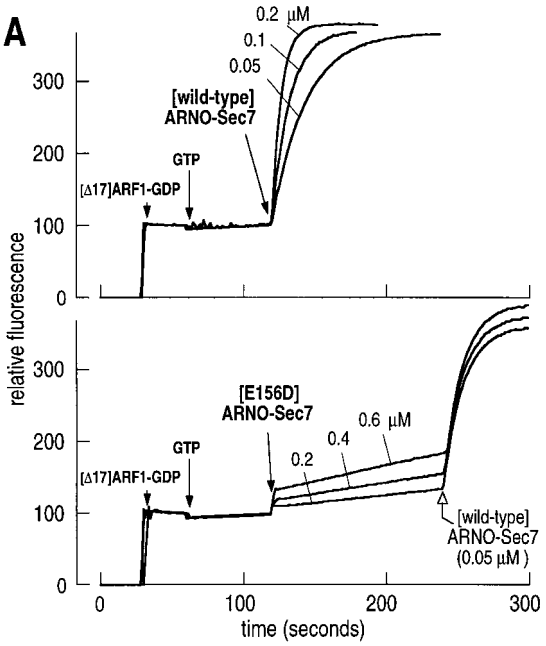

B

ARNO-Sec7	exchange activity $k_{exchange}$ /[Sec7] (10^5 s^{-1} M^{-1})	relative activity (%)
wild-type	7.6 ± 0.2	100
E117K	9.8 ± 0.6	129
W149Q	6.6 ± 0.4	87
R152E	1.4 ± 0.2	18
E156K	0.0065 ± 0.0002	0.085
E156D	0.020 ± 0.002	0.26
D183K	0.34 ± 0.02	4.5
M194A	0.14 ± 0.01	1.8
N201A	1.3 ± 0.1	17

Fig. 2. Effect of the conservative E156D mutation on the exchange activity of ARNO-Sec7 on [Δ17]ARF1. (**A**) The large tryptophan fluorescence change that accompanies the conformational change of ARF1 from the inactive, GDP-bound state to the active, GTP-bound state was used to follow in real-time the activation of [Δ17]ARF1 by wild-type ARNO-Sec7 or [E156D]ARNO-Sec7. The experiments were performed with 1 μM [Δ17]ARF1-GDP in a buffer containing 1 mM free Mg^{2+}. The reaction was initiated by the addition of 250 μM GTP and the indicated concentration of wild-type ARNO-Sec7 or [E156D]ARNO-Sec7. (**B**) Exchange activity of various ARNO-Sec7 mutants on [Δ17]ARF1. For each mutant, experiments similar to that shown in (A) were performed to determine the value ± SE of the specific exchange activity ($k_{exchange}$/[SEC7]), which corresponds to the rate constant of the activation of [Δ17]ARF1 normalized to the concentration of ARNO-Sec7 (see Materials and methods). Except for [E156K]ARNO-Sec7, the mutants were used at a concentration of up to 0.6 μM. For the E156K mutant, a very weak stimulation of [Δ17]ARF1 activation was detectable by varying the concentration of [E156K]ARNO-Sec7 from 1 to 5 μM.

Sec7 was incubated with a stoichiometric amount of the GDP-bound form of [Δ17]ARF1 and the mixture was loaded on a Superose 12 column. The experiment was performed in the presence of 1 μM or 1 mM free Mg^{2+}. Almost no interaction between [E156K]ARNO-Sec7 and [Δ17]ARF1 was detected at 1 mM Mg^{2+} (Figure 3). However, when the concentration of Mg^{2+} was reduced to 1 μM, [Δ17]ARF1 was almost entirely associated with [E156K]ARNO-Sec7. Thus, provided that the concentration of Mg^{2+} is low, the E156K mutation does not prevent the Sec7 domain from interacting with [Δ17]ARF1.

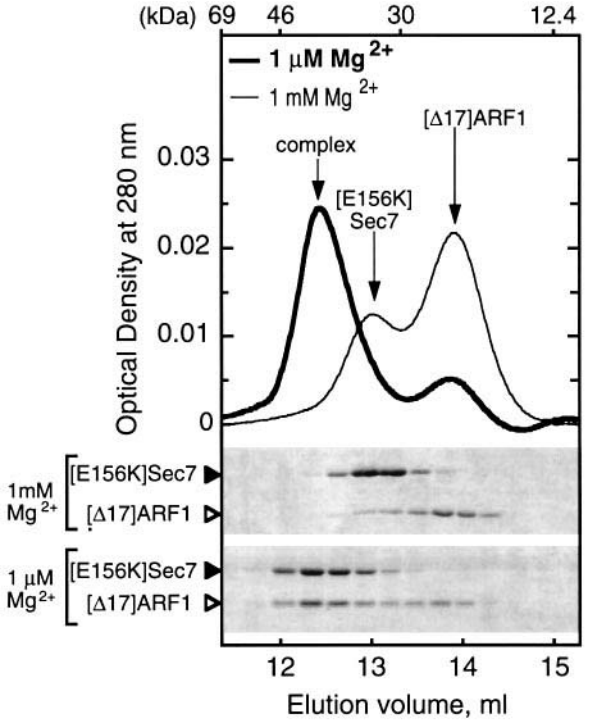

Fig. 3. [E156K]ARNO-Sec7 interacts with [Δ17]ARF1 at low Mg^{2+} concentration. The GDP-bound form of [Δ17]ARF1 (10 μM) was incubated with an equimolar amount of [E156K]ARNO-Sec7 in a buffer containing 1 μM or 1 mM free Mg^{2+}. Then the mixture was applied to a Superose 12 column equilibrated with the same buffer. The eluted fractions were analyzed for the presence of [Δ17]ARF1 and [E156K]ARNO-Sec7 by SDS–PAGE. The positions of molecular weight standards are shown.

Binding of wild-type ARNO-Sec7 to [Δ17]ARF1-GDP occurs at both 1 μM and 1 mM Mg^{2+} and promotes the dissociation of GDP (Paris *et al*., 1997). Conversely, an excess of GDP in the running buffer counteracts the formation of the stable nucleotide-free complex (Paris *et al*., 1997). This inhibitory effect of GDP was not observed with [E156K]ARNO-Sec7 (data not shown), suggesting that the binding of [E156K]ARNO-Sec7 does not promote the dissociation of GDP from [Δ17]ARF1. To test this hypothesis, gel filtration experiments were performed with [^{3}H]GDP-labeled [Δ17]ARF1 (Figure 4). The elution profile of the radiolabeled nucleotide was compared with that of [Δ17]ARF1, either isolated or in complex with wild-type ARNO-Sec7 or [E156K]ARNO-Sec7. [^{3}H]GDP co-eluted with [Δ17]ARF1 not only when [Δ17]ARF1 was isolated but also when [Δ17]ARF1 was complexed to [E156K]ARNO-Sec7 (Figure 4). In contrast, no GDP was associated with the complex between wild-type ARNO-Sec7 and [Δ17]ARF1. The complex between [Δ17]ARF1 and [E156K]ARNO-Sec7 at low Mg^{2+} concentration is therefore an abortive ternary complex in which GDP remains bound to the nucleotide-binding site. This result points to an essential role for Glu156 in the mechanism ARNO-Sec7-catalyzed GDP dissociation.

Among all ARNO-Sec7 mutants that display an impaired exchange activity on ARF1 (Cherfils *et al*., 1998; Figure 2B), the E156K mutant is the only one for which no correlation was found between the exchange activity

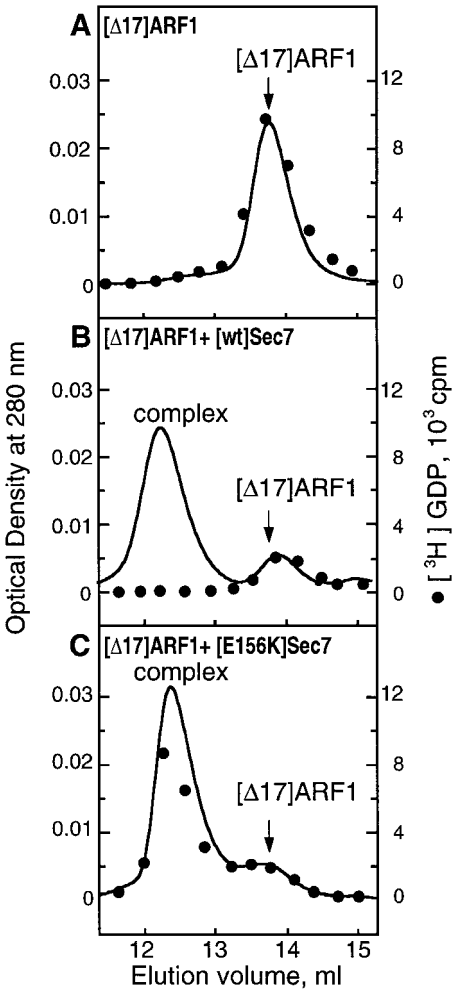

Fig. 4. The binding of [E156K]ARNO-Sec7 to [Δ17]ARF1-GDP at low Mg^{2+} concentration does not promote GDP dissociation. [^{3}H]GDP-labeled [Δ17]ARF1-GDP either (**A**) alone, or mixed with (**B**) an equimolar amount of wild-type ARNO-Sec7 or (**C**) [E156K]ARNO-Sec7 was incubated in a buffer containing 1 μM free Mg^{2+}. The various mixtures were then loaded on the gel filtration column equilibrated with the same low Mg^{2+} buffer. The eluted fractions were analyzed for the presence of [^{3}H]GDP. The experimental conditions were as in Figure 3. Note that [^{3}H]GDP co-elutes with [Δ17]ARF1 when the protein is alone or complexed to [E156K]ARNO-Sec7 but is released from [Δ17]ARF1 in the complex with wild-type ARNO-Sec7.

and the ability to form a complex with [Δ17]ARF1. For instance, under the experimental conditions used in Figure 3, the M194A mutant of ARNO-Sec7, which has a 50-fold reduced exchange activity on ARF1, did not form a complex with [Δ17]ARF at either 1 μM or 1 mM Mg^{2+} (data not shown). Furthermore, no complex was observed with the E156D mutant of ARNO-Sec7, suggesting that the positive charge of lysine in the E156K mutant is necessary for the formation of the abortive ternary complex. This could explain the observed inhibitory effect of Mg^{2+} on the formation of the complex between [Δ17]ARF1-GDP and [E156K]ARNO-Sec7 (Figure 3). As for any small G protein, Mg^{2+} interacts with the β-phosphate of the bound GDP in the nucleotide-binding site of ARF1 and strengthens the nucleotide–protein interaction (Greasley *et al*., 1995). As measured by a [^{3}H]GDP dissociation assay at various Mg^{2+} concentrations, the affinity of Mg^{2+} for [Δ17]ARF1-GDP is ~20 μM (data not shown) compared with a value of 2.8 μM for the affinity of Mg^{2+} for Ras-GDP (John *et al*., 1993). Thus, Mg^{2+} is bound to the nucleotide-binding site of [Δ17]ARF1-GDP at 1 mM but not at 1 μM Mg^{2+}. As Mg^{2+} inhibits the interaction between [Δ17]ARF1-GDP and [156K]ARNO-Sec7, this could indicate that the positive charge of Lys156 in [E156K]ARNO-Sec7 might replace Mg^{2+} in the nucleotide-binding site of [Δ17]ARF1-GDP. Conversely, this would imply that Glu156 in wild-type ARNO-Sec7 acts on Mg^{2+} or at least in the vicinity of the β-phosphate- and Mg^{2+}-binding sites of ARF1.

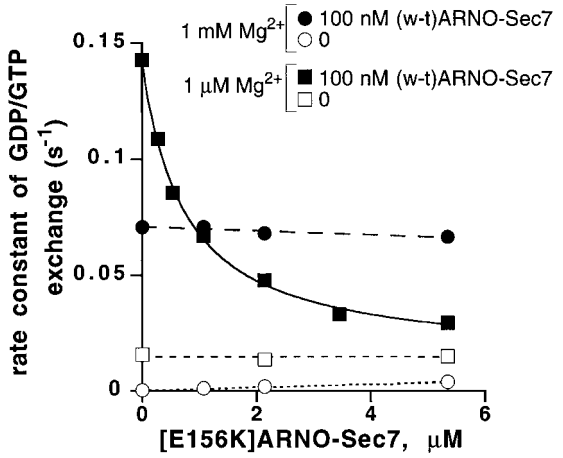

Fig. 5. Determination of the affinity of [E156K]ARNO-Sec7 for [Δ17]ARF1-GDP by competition experiments. [Δ17]ARF1-GDP (0.5 μM) was incubated with (●,■) or without (○,□) 100 nM wild-type ARNO-Sec7 and with increasing concentrations of [E156K]ARNO-Sec7 in a buffer containing 1 μM (□,■) or 1 mM (○,●) free Mg^{2+}. Then, GTP (250 μM) was added and the time course of [Δ17]ARF1 activation was followed by recording tryptophan fluorescence. The apparent rate constant of [Δ17]ARF1 activation upon GDP/GTP exchange activation was plotted as a function of [E156K]ARNO-Sec7 concentration. The hyperbolic fit for the experiment in the presence of wild-type ARNO-Sec7 at 1 μM Mg^{2+} (■) yields an apparent K_i of 0.7 μM.

The affinity of [E156K]ARNO-Sec7 for [Δ17]ARF1-GDP was determined by competition experiments. Catalysis of GDP/GTP exchange on [Δ17]ARF1 by a fixed amount of wild-type ARNO-Sec7 was measured in the presence of increasing concentrations of the E156K mutant (Figure 5). By sequestering the GDP-bound form of [Δ17]ARF1, this mutant inhibits Sec7-catalyzed nucleotide exchange on [Δ17]ARF1, with a K_i of 0.7 ± 0.1 μM. The inhibitory effect was observed at 1 μM Mg^{2+} but not at 1 mM Mg^{2+}, confirming that [E156K]ARNO-Sec7 does not interact with the Mg^{2+}-bound form of [Δ17]ARF1-GDP. It must be noted that at 1 μM Mg^{2+}, the rate of spontaneous GDP/GTP exchange on [Δ17]ARF1 was not affected by the presence of [E156K]ARNO-Sec7 (Figure 5). Thus, if [E156K]ARNO-Sec7 does not promote the release of the bound GDP from [Δ17]ARF1, neither does it slow down its spontaneous dissociation.

Exposed hydrophobic residues of the switch I region of ARF1 are involved in the interaction with ARNO-Sec7

Glu156 is at the edge of the hydrophobic groove of the Sec7 domain which, according to other mutations (R152E, M194A, N201A), participates in the interaction of ARNO-

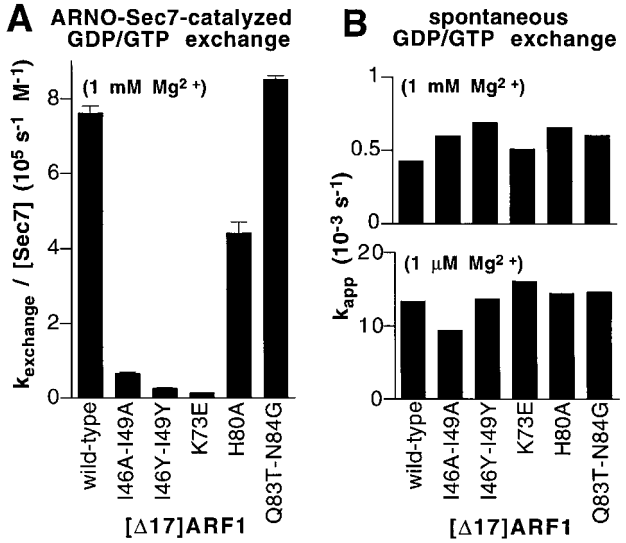

Fig. 6. Effect of point mutations in the switch I and switch II regions of [Δ17]ARF1 on the Sec7-catalyzed GDP/GTP exchange reaction. (**A**) Exchange activity of the Sec7 domain of ARNO on various [Δ17]ARF1 mutants. For each [Δ17]ARF1 mutant, kinetic experiments similar to that shown in Figure 2A were carried out in the presence of various concentrations of the Sec7 domain. The relative sensitivity of each [Δ17]ARF1 mutant to ARNO-Sec7 was determined by comparing the specific exchange activity values ($k_{exchange}$/[SEC7]). (**B**) Rate constant of the spontaneous GDP/GTP exchange of each mutant at 1 mM and 1 μM free Mg^{2+}.

Sec7 with ARF1 (Cherfils *et al*., 1998; Figures 1 and 2). Since Glu156 might contact the Mg^{2+} ion and the β-phosphate of GDP bound to ARF1, the hydrophobic groove of the Sec7 domain could serve as a binding pocket for exposed hydrophobic residues of ARF1 that are close to the β-phosphate- and Mg^{2+}-binding sites. Candidate residues are found in the switch I region of ARF1. This region, which is formed by the 'extra' β2E strand and the following loop, contains three exposed hydrophobic residues (Val43, Ile46 and Ile49) which together form an extended hydrophobic protuberance (Figure 1).

To investigate the role of the switch I region of ARF1 in the interaction with ARNO-Sec7, Ile46 and Ile49 of [Δ17]ARF1 were both replaced by alanines or tyrosines. The latter substitution was chosen because tyrosine is a bulky hydrophilic residue and is commonly found in β-strands. As shown in Figure 6A, the I46A-I49A and the I46Y-I49Y mutations reduced the sensitivity of [Δ17]ARF1 to the exchange activity of ARNO-Sec7 by factors of 10 and 25, respectively. In contrast, these mutations only slightly modified the rate of spontaneous GDP/GTP exchange at both low and high Mg^{2+} levels, suggesting that they do not affect the Mg^{2+}- and nucleotide-binding sites (Figure 6B). Therefore, Ile46 and/or Ile49 are probably involved in the interaction with ARNO-Sec7. The fact that the replacement of Ile46 and Ile49 by tyrosines had a more pronounced effect than their replacement by alanines suggests that the region of ARNO-Sec7 that interacts with I46 and I49 of ARF1 can accommodate the small hydrophobic side chain of alanine more easily than the bulky hydrophilic side chain of tyrosine.

Lys73 of the switch II region of ARF1 and Asp183 of the Sec7 domain of ARNO form an ion pair

The elongated shape of the switch I region of ARF1 suggests that it could insert into the hydrophobic groove of ARNO-Sec7 with the axis of strand β2E parallel to the main axis of the groove (Figure 1). Although two opposite orientations are possible, only one of them positions the β-phosphate and the coordinated Mg^{2+} of ARF1-GDP near the 'catalytic' Glu156 residue of the Sec7 domain. Interestingly, this orientation suggests that the N-terminal part of the switch II region of ARF1 could also participate in the interaction with the Sec7 domain. The switch II region of ARF1 consists of loop L4, helix α2 and loop L5. Loop L4, which is poorly defined in the crystal structure of ARF1-GDP, contains a highly exposed basic residue (Lys73). This residue lies at the end of the elongated protuberance formed by Ile46 and Ile49 (Figure 1).

We reported previously that mutation of Lys73 in full-length myristoylated ARF1 abolishes the ability of ARNO to stimulate nucleotide exchange (Cherfils *et al*., 1998). This mutation was also introduced in [Δ17]ARF1, and its effect on the Sec7-catalyzed nucleotide exchange reaction was compared with the effect induced by mutations in more distal parts of the switch II region: H80A in the central α2 helix and Q83T-N84G in the following L5 loop. The H80A and Q83T-N84G mutants of [Δ17]ARF1 were activated by wild-type ARNO-Sec7 nearly as well as the wild-type form of [Δ17]ARF1 (Figure 6A). In contrast, a 60-fold decrease in the rate of Sec7-catalyzed GDP/GTP nucleotide exchange was observed for the K73E mutant, although this mutant displayed spontaneous GDP/GTP exchange kinetics similar to those observed for wild-type [Δ17]ARF1 (Figure 6B). Thus, the N-terminal part (Lys73) but not the central (His80) and the C-terminal parts (Gln83, Asn84) of the switch II region seem to be involved in the interaction of ARF1 with the Sec7 domain of ARNO.

The insertion of Ile46 and Ile49 of ARF1 into the hydrophobic groove of ARNO-Sec7 would position the adjacent Lys73 residue near a patch of three acidic residues (Asp161, Glu165 and Asp183) that forms one end of the groove (Figure 1). Since Asp183 of ARNO is strictly conserved in the Sec7 family (Chardin *et al*., 1996), we suspected that this residue could form an ion pair with Lys73 of ARF1. The existence of this putative ion pair was investigated by charge permutation between Lys73 (ARF1) and Asp183 (ARNO-Sec7). Asp183 in ARNO-Sec7 was mutated to lysine and assayed for its exchange activity on wild-type [Δ17]ARF1 and on the K73E mutated form of [Δ17]ARF1 (Figure 7A). Compared with ARNO-Sec7, [D183K]ARNO-Sec7 displayed a 20-fold reduced exchange activity when tested on wild-type [Δ17]ARF1. This identifies Asp183 as another residue close to the groove of the Sec7 domain that contributes to the binding of ARF1 (see Figure 2B for a comparison with other ARNO-Sec7 mutants). In contrast, [D183K]ARNO-Sec7 was four times more active than wild-type ARNO-Sec7 when tested on the K73E mutated form of [Δ17]ARF1. Thus, the effects of the two charge reversal mutations were not additive but, on the contrary, partially compensated (Figure 7B), suggesting that in the ARF1–ARNO-Sec7 interface, Lys73 of ARF1 and Asp183 of ARNO-Sec7 form an ion pair.

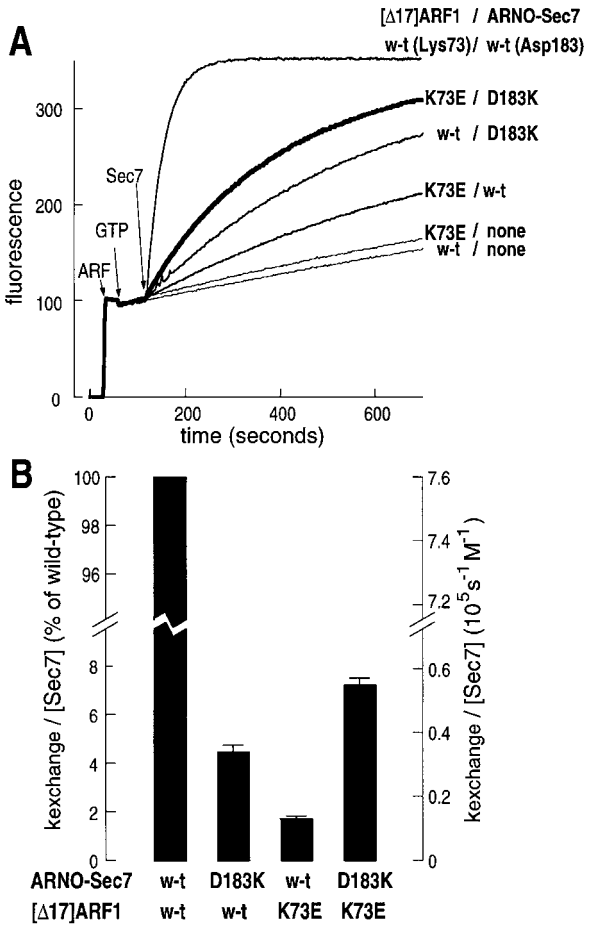

Fig. 7. Charge reversal mutations reveal an ion pair interaction between Lys73 of ARF1 and Asp183 of the Sec7 domain of ARNO. (**A**) The activation of the wild-type form or the K73E mutated form of [Δ17]ARF1-GDP (1 μM) was measured by tryptophan fluorescence. When indicated, GTP (250 μM) and ARNO-Sec7 (50 nM), either mutated (D183K) or not, were added. As a control, the same experiment was performed in the absence of ARNO-Sec7. (**B**) Plot of the relative and absolute values of specific exchange activity ($k_{exchange}$/[SEC7]) for the four pairs of [Δ17]ARF and ARNO-Sec7 proteins.

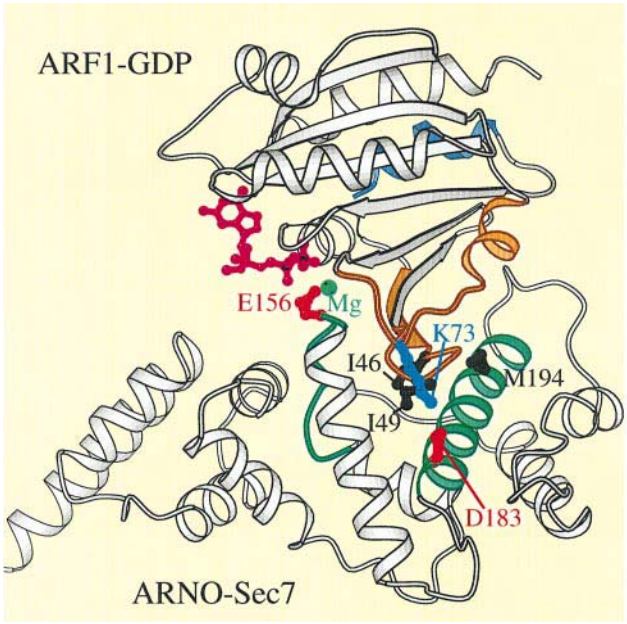

Fig. 8. Model for the interaction of ARNO-Sec7 with ARF1-GDP. Color coding is as in Figure 1. The orientation of ARNO-Sec7 is approximately the same as in Figure 1, but ARF1-GDP has been rotated by ~30° around a vertical axis. The model was built using the experimentally identified contacts between ARNO-Sec7 and ARF1: Glu156 (ARNO-Sec7)/Mg^{2+} (ARF1-GDP), Asp183 (ARNO-Sec7)/Lys73 (ARF1-GDP), and the hydrophobic contact between the groove of ARNO-Sec7 and the switch I of ARF1 (see Materials and methods). The model aligns the switch I of ARF1 and the hydrophobic groove of ARNO-Sec7. The ion pair between Lys73 of ARF1 and Asp183 of ARNO-Sec7 is the only contribution of the switch II to the interface; however, this region is flexible in ARF1-GDP and may reorganize to yield larger contacts. Except for its interaction with E156 in ARNO-Sec7, the GDP nucleotide is essentially as exposed to the solvent as it is in isolated ARF1-GDP. This is compatible with the formation of a nucleotide-free intermediate complex. Note that only minor side chain modifications were required to achieve a model with reasonable complementarity and that no attempt was made to modify the orientation of any region of ARF1 towards the core domain of the protein. However, a structural change in strand β2E might link the binding of ARNO-Sec7 to the destabilization of the N-terminal helix by membrane lipids. This figure was generated with MOLSCRIPT (Kraulis, 1991).

Discussion

Two observations establish the spatial relationship between the switch regions of ARF1 and the active site of ARNO-Sec7: (i) the formation of an abortive ternary complex between [E156K]ARNO-Sec7 and the Mg^{2+}-free form of [Δ17]ARF1-GDP suggests that the carboxylate group of Glu156 points toward the Mg^{2+} and β-phosphate in the nucleotide-binding site of ARF1; and (ii) the partial compensation of two charge reversal mutations, K73E in ARF1 and D183K in ARNO-Sec7, suggests that these residues form an ion pair. These two contacts provide strong guiding constraints for docking ARF1-GDP onto ARNO-Sec7 and were used to build a model for the ternary complex between ARNO-Sec7, ARF1 and the GDP nucleotide (Figure 8). In this model, the extra β2E strand of the switch I region of ARF1 fills the characteristic hydrophobic groove of the Sec7 domain, consistent with the fact that mutations that reduce the hydrophobicity of the groove in ARNO-Sec7 or that of the switch I region in [Δ17]ARF1 impair the functional interaction between the two proteins. The complementarity of molecular shapes suggests that several hydrophobic residues are engaged in the contact, including Val43, Ile46 and Ile49 from ARF1 and Ala157, Ile160, Phe190 and Met194 from ARNO-Sec7. The switch II of ARF1 contributes to the interface only by the potential salt bridge between Lys73 of ARF1 and Asp183 of ARNO. This interaction may cause the switch II to take on a more stable conformation than in the ARF1-GDP complex, eventually yielding a larger contact with ARNO-Sec7. Altogether, these protein–protein contacts position Glu156 of the Sec7 domain near the Mg^{2+} and the β-phosphate of the bound GDP.

While this work was in progress, Mossessova *et al.* (1998) have shown that the switch regions of [Δ17]ARF1 are protected from hydroxyl radical-mediated cleavage by the binding of ARNO-Sec7. This footprinting method gives a large map of the surface of ARF1 that interacts with ARNO-Sec7, but with a low resolution. Our mutagenesis study details the various amino acids involved in the ARF1–Sec7 interface and, more importantly, permits docking of the two proteins and the assignment of a role to some residues, either in the protein–protein interface or in the mechanism of nucleotide exchange.

At a low Mg^{2+} concentration, the E156K Sec7 mutant forms a complex with [Δ17]ARF1-GDP without inducing the release of the bound GDP (Figures 3 and 4). To our knowledge, this is the first example of an abortive ternary complex between a small-GTP binding protein, a bound nucleotide (GDP) and a nucleotide exchange factor. This complex might mimic the ternary complex that precedes the dissociation of GDP and the formation of the stable and binary nucleotide-free complex. As shown by kinetic and equilibrium studies on the interaction of the small GTP-binding protein Ran with its exchange factor RCC1, such a ternary complex is a highly transient intermediate of the reaction scheme (Klebe *et al*., 1995b). An intriguing observation is that the abortive complex between [E156K]Arno-Sec7 and [Δ17]ARF1-GDP does not form when GDP is coordinated to Mg^{2+}. This suggests that the amino group of Lys156, in the E156K mutant, might occupy the Mg^{2+} binding-site, provided that this site is empty, as is the case at 1 μM Mg^{2+}.

As shown by the E156K and E156D mutations, the catalytic function of Glu156 depends on both its carboxylic group and the length of its side chain. Thus we propose that Glu156 acts as a 'glutamic finger'. In a first step, the carboxylic group of Glu156 may interact with Mg^{2+} and destabilize the coordinations of Mg^{2+} with the β-phosphate of GDP, hence favoring the dissociation of the nucleotide. However, other contributions must be considered to account for the actual catalytic efficiency. ARNO-Sec7 accelerates GDP/GTP exchange on [Δ17]ARF1 by a factor of at least 2×10^4 (k_{cat} >10/s) whereas removal of Mg^{2+} by EDTA accelerates GDP/GTP exchange by only a factor of 20 (k_{off}GDP ≈10^{-2}/s and 5×10^{-4}/s at 1 μM and 1 mM Mg^{2+}, respectively; Figure 6B). Moreover, the conservative mutation E156D impairs the exchange activity of ARNO-Sec7 not only at 1 mM Mg^{2+} but also at 1 μM (data not shown), suggesting that the role of Glu156 is not limited to the destabilization of Mg^{2+}. The removal of Mg^{2+} would leave Glu156 in a repulsive environment of negative charges from the GDP phosphates and several aspartic residues. We suggest that in a second step of the mechanism, Glu156 may contribute to the release of the nucleotide by repulsion of the negative charges of the phosphates in GDP. Finally, in the stable and nucleotide-free binary complex between ARF1 and ARNO-Sec7, the carboxylate of Glu156 might mimick the β-phosphate of GDP in the nucleotide-binding site of ARF1, turning the repulsive effect towards GDP into a stabilizing interaction with ARF1. Structural equivalence of carboxylates with phosphates is not uncommon in proteins, as engineered in isocitrate dehydrogenase for instance (Hurley *et al*., 1990).

In our model, the N-terminal helix of ARF1 makes no contact with ARNO-Sec7 (Figure 8). This is in agreement with our previous observation that [Δ17]ARF1, which lacks the N-terminal helix, interacts with and is activated by ARNO-Sec7 (Paris *et al*., 1997). This is also consistent with the fact that all mutations that impair the exchange activity of ARNO-Sec7 on full-length myristoylated ARF1 (Cherfils *et al*., 1998) have the same effect on [Δ17]ARF1 (Figure 2B). However, the N-terminal helix of ARF1, which is myristoylated and amphipathic, plays a major role in the nucleotide exchange process by interacting with membrane lipids (Franco *et al*., 1995, 1996; Antonny *et al*., 1997; Paris *et al*., 1997). In the absence of lipids, stimulation of the dissociation of GDP from full-length myristoylated ARF1 by ARNO or by the Sec7 domain of ARNO is barely detectable (Paris *et al*., 1997). The insertion of the myristate into the bilayer and electrostatic interactions between basic residues and anionic lipids might destabilize the N-terminal helix from the core domain of ARF1-GDP and trigger a conformational change in ARF1-GDP that could facilitate its interaction with ARNO-Sec7. In the crystal structure of non-myristoylated ARF1-GDP, the hydrophobic face of the N-terminal helix is packed against several hydrophobic residues of the core domain of ARF1 including Leu37 and Leu39 (Amor *et al*., 1994; Greasley *et al*., 1995). These two residues belong to the loop that precedes strand β2E. Thus, they are structurally connected through strand β2E to residues such as Ile46 and Ile49, which participate in the interaction of ARF1 with the Sec7 domain. Therefore, strand β2E might serve as a linker to coordinate the destabilization of the N-terminal helix of ARF1-GDP by membrane lipids with the binding of ARNO-Sec7 to ARF1-GDP.

Can we extend the model proposed here to the interaction of other small GTP-binding proteins with their GEFs? Several studies have shown that the switch I (Burstein *et al*., 1992; Li and Zheng, 1997) and/or switch II (Verrotti *et al*., 1992; Quilliam *et al*., 1996) regions of the small GTP-binding proteins Ras, Rho and Rab participate in the interaction with GEFs. However, the identified critical regions overlap only partially with those of ARF1. For instance, the distal region of the switch II region (helix α2 and the following loop) is critical for the interaction of Ras with CDC25, a Ras GEF (Verrotti *et al*., 1992), but not for the interaction of ARF1 with ARNO-Sec7 (Figure 6). In addition, the unrelated structures of ARNO-Sec7 (Cherfils *et al*., 1998) and RCC1, the exchange factor for Ran (Renault *et al*., 1998), do not argue in favor of a general recognition mechanism between GEFs and small GTP-binding proteins, yet local binding and catalytic features may be common. Rho and Rab proteins display, in the switch I region, several hydrophobic residues which participate in the interaction with their exchange factors (Burstein *et al*., 1993; Li and Zheng, 1997). In Ras, the flexible L4 loop of the switch II region contains a glutamate residue (Glu63) which, according to a complementary genetic approach, interacts with a conserved arginine residue of the CDC25 nucleotide exchange factor (Park *et al*., 1994). In terms of a catalytic mechanism, the only model available so far derives from the crystal structure of the G protein EF-Tu in complex with its exchange factor EF-Ts. Although EF-Ts binds to the switch II region of EF-Tu and destabilizes the bound GDP by acting on the Mg^{2+}- and β-phosphate binding sites, its mode of binding is unrelated to our model and the mechanism of catalysis does not involve a glutamate residue (Kawashima *et al*., 1996; Wang *et al*., 1997). Acidic residues, on the other hand, have been associated with other nucleotide exchange factor mechanisms. A genetic approach identified a conserved aspartate (Asp266) of a CDC25-like exchange factor for Ras as a key catalytic residue (Camus *et al*., 1995). In RCC1 too, aspartate residues (Asp128 and Asp182) have been involved in the GEF activity (Azuma *et al*., 1996). Thus it is possible that acidic residues will be endowed with catalytic functions similar to Glu156 of ARNO-Sec7 in other GEFs.

Materials and methods

Site-directed mutagenesis

The QuickChange site-directed mutagenesis kit of Stratagene was used to make point mutations in the genes of [Δ17]ARF1 and ARNO-Sec7 cloned in pET-11d plasmids (Novagen). The complementary primers containing the desired mutation were between 26 and 39 bases in length. The sequence of each mutant was verified by automated sequencing.

Protein expression and purification

[Δ17]ARF1, a truncated form of ARF1 lacking the first 17 N-terminal amino acids, and ARNO-Sec7 (residues 50–252 of ARNO) were expressed in *Escherichia coli* as previously described (Chardin *et al*., 1996; Antonny *et al*., 1997). For the purification of ARNO-Sec7, bacteria were lysed for 30 min at 4°C in 50 mM Tris pH 7.5, 1 mM EDTA, 1 mM dithiothreitol (DTT) supplemented with lyzozyme (1 g/l), and a cocktail of antiproteases (Boehringer Mannheim). Then 5 mM $MgCl_2$, 100 μg/ml DNase and 0.02% deoxycholate were added for an additional 30 min. The suspension was centrifuged for 90 min at 400 000 *g* and the supernatant was applied to a Q Sepharose fast-flow column (1.6×20 cm) equilibrated in 50 mM Tris pH 7.5, 5 mM $MgCl_2$, 1 mM EDTA and 1 mM DTT. The Sec7 domain was purified using a linear (0–1 M) NaCl gradient. Fractions containing ARNO-Sec7 were pooled and stored at –80°C. For the purification of [Δ17]ARF1, bacteria were resuspended in 50 mM Tris pH 7.5, 100 mM NaCl, 1 mM $MgCl_2$, 0.4 mM phenylmethylsulfonyl fluoride (PMSF) and 1 mM DTT supplemented with 200 μM GDP. Cells were lysed using a French press, and [Δ17]ARF1-GDP was purified from the soluble extract by gel filtration (Sephacryl S200 HR, Pharmacia) in 50 mM Tris pH 7.5 and 1 mM $MgCl_2$. Fractions containing [Δ17]ARF1 were concentrated on an Amicon cell and stored at –80°C. As determined by SDS–PAGE, [Δ17]ARF1-GDP and ARNO-Sec7 were 90 and ~70% pure, respectively.

Gel filtration

Complex formation between ARNO-Sec7 and [Δ17]ARF1 was analyzed by gel filtration. All experiments were performed at room temperature on a Superose 12 HR column (1×30 cm, Pharmacia). The running buffer contained 20 mM Tris pH 7.5, 100 mM NaCl, 1 mM $MgCl_2$, 5 mM β-mercaptoethanol and 0.1 mM PMSF. Where indicated, this buffer was supplemented with 2 mM EDTA to reduce the concentration of free magnesium to ~1 μM. [Δ17]ARF1-GDP (10 μM) was incubated with or without ARNO-Sec7 (10 μM) in the running buffer for 10 min at room temperature. Then 200 μl of the sample was applied to the column at a flow rate of 0.5 ml/min, and the optical density at 280 nm was recorded continuously. Fractions of 0.3 ml were collected and 60 μl of each fraction were analyzed by SDS–PAGE with Coomassie Blue staining. When [^{3}H]GDP-labeled [Δ17]ARF1 was used, radioactivity was determined by counting 50 μl aliquots of each fraction.

Kinetic measurements

Activation of [Δ17]ARF1 upon GDP/GTP exchange was measured by tryptophan fluorescence (Antonny *et al*., 1997). All measurements were performed at 37°C in 50 mM HEPES pH 7.5, 100 mM KCl, 1 mM $MgCl_2$ and 2 mM DTT. When indicated, the buffer was supplemented with EDTA (2 mM) to reduce the concentration of free Mg^{2+} to 1 μM. The apparent rate constant of [Δ17]ARF1 activation (k_{app}) was determined by fitting the fluorescence change with a single exponential and plotted as a function of [ARNO-Sec7]. k_{app} increases linearly with the concentration of ARNO-Sec7 according to the equation:

$$k_{app} = a + b[\text{ARNO-Sec7}]$$

where a is the rate constant of the spontaneous nucleotide exchange, which was measured in the absence of ARNO-Sec7, and b is the specific exchange activity of ARNO-Sec7, i.e. the rate constant of the catalyzed GDP/GTP exchange normalized to the concentration of ARNO-Sec7 ($k_{exchange}$/[ARNO-Sec7]). This parameter corresponds to the apparent second order rate constant k_{cat}/K_m of a Michaelis–Menten mechanism. Note that we did not determine the individual k_{cat} and K_m values. At a constant concentration of wild-type ARNO-Sec7 (100 nM), the rate of [Δ17]ARF1 activation did not saturate and remained nearly linear for concentrations of [Δ17]ARF1-GDP up to 10 μM. Thus, at least for the reaction between wild-type ARNO-Sec7 and wild-type [Δ17]ARF1-GDP, only lower limits for the k_{cat} and K_m values can be given: K_m >10 μM and k_{cat} >10/s.

Model building of the ARNO-Sec7–ARF1-GDP complex

The model was built from the crystal structures of human ARNO-Sec7 (Cherfils *et al*., 1998) and ARF1-GDP (Amor *et al*., 1994; PDB entry 1HUR) by manually placing Glu156 and Asp183 in the proximity of the Mg^{2+}-binding site and Lys73 of ARF1, respectively. These constraints left essentially a rotational degree of freedom, which was solved by the complementarity in shape and hydrophobicity between the switch I of ARF1 and the groove of ARNO-Sec7. The model was then refined by rigid body docking, followed by manual adjustment of several side chains (including E156 and D183 of ARNO-Sec7 and K73 of ARF1). The model finally was subjected to energy minimization.

Acknowledgements

This work was supported in parts by grants from the CNRS (Biologie Cellulaire, Grant 96 121). P.C. is supported by INSERM.

References

Amor,J.C., Harrison,D.H., Kahn,R.A. and Ringe,D. (1994) Structure of the human ADP-ribosylation factor 1 complexed with GDP. *Nature*, **372**, 704–708.

Antonny,B., Béraud-Dufour,S., Chardin,P. and Chabre,M. (1997) N-terminal hydrophobic residues of the G-protein ADP-ribosylation factor-1 insert into membrane lipids upon GDP to GTP exchange. *Biochemistry*, **36**, 4675–4684.

Azuma,Y., Seino,H., Seki,T., Uzawa,S., Klebe,C., Ohba,T., Wittinghofer,A., Hayashi,N. and Nishimoto,T. (1996) Conserved histidine residues of RCC1 are essential for nucleotide exchange on Ran. *J. Biochem.*, **120**, 82–91.

Burstein,E.S., Brondyk,W.H. and Macara,I.G. (1992) Amino acid residues in the ras like GTPase Rab3A that specify sensitivity to factors that regulate the GTP/GDP cycling of Rab3A. *J. Biol. Chem.*, **267**, 22715–22718.

Camus,C., Herrmann-Le Denmat,S. and Jacquet,M. (1995) Identification of guanine exchange factor key residues involved in exchange activity and Ras interaction. *Oncogene*, **11**, 951–959.

Chardin,P., Paris,S., Antonny,B., Robineau,S., Béraud-Dufour,S., Jackson,C.L. and Chabre,M. (1996) A human exchange factor for ARF contains Sec7- and pleckstrin-homology domains. *Nature*, **384**, 481–484.

Cherfils,J., Ménétray,J. Mathieu,M., Le Bras,G., Robineau,S., Béraud-Dufour,S., Antonny,B. and Chardin,P. (1998) Structure of the Sec7 domain of the Arf exchange factor ARNO. *Nature*, **392**, 101–105.

Franco,M., Chardin,P., Chabre,M. and Paris,S. (1993) Myristoylation is not required for GTP-dependent binding of ADP-ribosylation factor 1 to phospholipids. *J. Biol. Chem.*, **268**, 24531–24534.

Franco,M., Chardin,P., Chabre,M. and Paris,S. (1995) Myristoylation of ADP-ribosylation factor 1 facilitates nucleotide exchange at physiological Mg^{2+} levels. *J. Biol. Chem.*, **270**, 1337–1341.

Franco,M., Chardin,P., Chabre,M. and Paris,S. (1996) Myristoylation-facilitated binding of the G protein $ARF1_{GDP}$ to membrane phospholipids is required for its activation by a soluble nucleotide exchange factor. *J. Biol. Chem.*, **271**, 1573–1578.

Greasley,S.E., Jhoti,H., Teahan,C., Solari,R., Fensome,A., Thomas,G.M.H., Cockcroft,S. and Bax,B. (1995) The structure of ADP-ribosylation factor-1 (ARF-1) complexed to GDP determined from two different crystal forms. *Nature Struct. Biol.*, **2**, 797–806.

Hurley,J.H., Dean,A.M., Sohl,J.L., Koshland,D.E. and Stroud,R.M. (1990) Regulation of an enzyme by phosphorylation at the active site. *Science*, **249**, 1012–1016.

Jacquet,E., Baouz,S., and Parmeggiani,A. (1995) Characterization of mammalian C-CDC25^{Mn} exchange factor and kinetic properties of the exchange reaction intermediate p21·C-CDC25^{Mn}. *Biochemistry*, **34**, 12347–12354.

John,J., Rensland,H., Schlichting,I., Vetter,I., Borasio,G.D., Goody,R.S. and Wittinghofer,A. (1993) Kinetic and structural analysis of the Mg^{2+}-binding site of the guanine nucleotide-binding protein $p21^{H\text{-}ras}$. *J. Biol. Chem.*, **268**, 923–929.

Kawashima,T., Berthet-Colominas,C., Wulff,M., Cusack,S. and Leberman,R. (1996) The structure of the EF-Tu·EF-Ts complex at 2.5 Å resolution. *Nature*, **379**, 511–518.

Klarlund,J.K., Rameh,L.E., Cantley,L.C., Buxton,J.M., Holik,J.J., Sakelis,C., Patki,V., Corvera,S. and Czech,M.P. (1998) Regulation of Grp1-catalyzed ADP ribosylation factor guanine nucleotide exchange

by phosphatidylinositol 3,4,5-trisphosphate. *J. Biol. Chem.*, **273**, 1859–1862.

Klebe,C., Bischoff,F.R., Ponstingl,H. and Wittinghofer,A. (1995a) Interaction of the nuclear GTP-binding protein Ran with its regulatory proteins RCC1 and RanGAP1. *Biochemistry*, **34**, 639–647.

Klebe,C., Prinz,H., Wittinghofer,A. and Goody,R.S. (1995b) The kinetic mechanism of Ran-nucleotide exchange catalyzed by RCC1. *Biochemistry*, **34**, 12543–12552.

Kraulis,P.J. (1991) MOLSCRIPT: a program to produce both detailed and schematic plots of protein structures. *J. Appl. Crystallogr.*, **24**, 946–950.

Li,R. and Zheng,Y. (1997) Residues of the Rho family GTPases Rho and Cdc42 that specify sensitivity to dbl-like guanine nucleotide exchange factors. *J. Biol. Chem.*, **272**, 4671–4679.

Meacci,E., Tsai,S.-C., Adamik,R., Moss,J. and Vaughan,M. (1997) Cytohesin-1, a cytosolic guanine nucleotide-exchange protein for ADP-ribosylation factor. *Proc. Natl Acad. Sci. USA*, **94**, 1745–1748.

Milburn,M.V., Tong,L., deVos,A.M., Brünger,A., Yamaizumi,Z., Nishimura,S. and Kim,S.-H. (1990) Molecular switch for signal transduction: structural differences between active and inactive forms of protooncogenic ras proteins. *Science*, **247**, 939–945.

Morinaga,N., Moss,J. and Vaughan,M. (1997) Cloning and expression of a cDNA encoding a bovine brain brefeldin A-sensitive guanine nucleotide-exchange protein for ADP-ribosylation factor. *Proc. Natl Acad. Sci. USA*, **94**, 12926–12931.

Moss,J. and Vaughan,M. (1995) Structure and function of ARF proteins: activators of cholera toxin and critical components of intracellular vesicular transport processes. *J. Biol. Chem.*, **270**, 12327–12330.

Mossessova,E., Gulbis,J.M. and Goldberg,J. (1998) Struture of the guanine nucleotide exchange factor Sec7 domain of human ARNO and analysis of the interaction with ARF GTPase. *Cell*, **92**, 415–423.

Pai,E.F., Krengel,U., Petsko,G.A., Goody,R.S., Kabsch,W. and Wittinghofer,A. (1990) Refined crystal structure of the triphosphate conformation of H-ras p21 at 1.35 Å resolution: implications for the mechanism of GTP hydrolysis. *EMBO J.*, **9**, 2351–2359.

Paris,S., Béraud-Dufour,S., Robineau,S., Bigay,J., Antonny,B., Chabre,M. and Chardin,P. (1997) Role of protein–phospholipid interactions in the activation of ARF1 by the guanine nucleotide exchange factor ARNO. *J. Biol. Chem.*, **272**, 22221–22226.

Park,W., Mosteller, R.D. and Broek,D. (1994) Amino acid residues in the CDC25 guanine nucleotide exchange factor critical for interaction with Ras. *Mol. Cell. Biol.*, **14**, 8117–8122.

Peyroche,A., Paris,S. and Jackson,C.L. (1996) Nucleotide exchange on ARF mediated by yeast Gea1 protein. *Nature*, **384**, 479–481.

Quilliam,L.A. *et al.* (1996) Involvement of the switch 2 domain of Ras in its interaction with guanine nucleotide exchange factors. *J. Biol. Chem.*, **271**, 11076–11082.

Renault,L., Nassar,N., Vetter,I., Becker,J., Klebe,C., Roth,M. and Wittinghofer,A. (1998) The 1.7 Å crystal structure of the regulator of chromosome condensation (RCC1) reveals a seven-bladed propeller. *Nature*, **392**, 97–101.

Verrotti,A.C. *et al*. (1992) Ras residues that are distant from the GDP binding site play a critical role in dissociation factor-stimulated release of GDP. *EMBO J.*, **11**, 2855–2862.

Wang,Y., Jiang,Y., Meyering-Voss,M., Sprinzl,M. and Sigler,P.B. (1997) Crystal structure of the EF-Tu·EF-Ts complex from *Thermus thermophilus*. *Nature Struct. Biol.*, **4**, 650–656.

Received March 27, 1998; revised April 28, 1998; accepted April 29, 1998